

Joint Trajectories and Power Allocation Design for Dual UAV-Enabled Secrecy SWIPT Networks

Feng Zhou^{1, 3, *}, Rugang Wang^{1, 2}, and Jinhong Bian^{1, 3}

Abstract—In this paper, a dual unmanned aerial vehicle (UAV)-enabled secure communication system with simultaneous wireless and information and power transfer (SWIPT) has been investigated. Specifically, assuming that the energy receivers (ERs) may be potential eavesdroppers (Eves), we aim to maximize the minimum secrecy rate among multiply legitimate receivers (LRs) within each period by jointly adjusting the UAVs' trajectories and power control (PC). Since the resulting optimization problem is very difficult to solve due to highly non-convex objective and constraints, we equivalently transform it into a more tractable problem via successive convex approximation (SCA) and constrained concave-convex procedure (CCCP), then propose an iterative method. The simulation results show that the proposed joint optimization algorithm achieves significantly better performance than the conventional algorithms.

1. INTRODUCTION

Over the past decades, the unmanned aerial vehicle (UAV)-aided wireless communications have attracted growing interest due to several advantages, such as being flexible on-demand deployment, controllable mobility, and line-of-sight (LoS) aerial-ground channel [1]. However, due to the openness and broadcast characteristic of the aerial-ground channel, security is an important issue for UAV communication [2]. The confidential information transmitted by the UAV to the ground station may be eavesdropped by the eavesdropper (Eve) [3]. Recently, secure UAV communication has aroused great attention, while joint trajectory and power allocation are widely investigated to improve the security in UAV networks [4].

Specifically, in [5], the authors investigated the joint trajectory and power allocation in secrecy UAV networks. In [6], the authors investigated a robust trajectory, and power allocation design with considering only imperfect Eve's location information can be obtained. In [7], the authors extended the previous work to multiple LRs and Eves case. In [8], the authors considered a practical factor that there exist several no-fly zones (NFZ) in the UAV's flight area and proposed a low complexity alternating directional method of multipliers (ADMM) method.

To further improve security, dual-UAV enabled secrecy network, e.g., one UAV transmit information and one UAV emit jamming signal, has aroused great attention. Specifically, in [9], the authors proposed a penalty constrained concave-convex procedure (P-CCCP) technique to jointly design the two UAVs' power and trajectories. In [10], the authors proposed a block successive upper bound minimization (BSUM) method to solve a similar problem. Recently, in [11], the authors proposed an alternating optimization (AO) and successive convex approximation (SCA) method. In [12], the authors proposed an efficient iterative algorithm by applying the block coordinate descent (BCD) and SCA techniques to find a high quality approximate solution.

Received 28 September 2019, Accepted 23 November 2019, Scheduled 6 December 2019

* Corresponding author: Feng Zhou (zfyct@ycit.edu.cn).

¹ School of Information Technology, Yancheng Institute of Technology, Yancheng 224051, China. ² Key Laboratory of Underwater Acoustic Signal Processing, Ministry of Education, Southeast University, Nanjing 210096, China. ³ Research Center of Photoelectric Technology, Yancheng Institute of Technology, Yancheng 224051, China.

On the other hand, the simultaneous wireless and information and power transfer (SWIPT) technique [13] is considered as an effective way to improve the energy efficiency in UAV networks. Recently, in [14], the authors investigated the joint trajectory and power allocation in secrecy UAV networks with SWIPT, where the energy receiver (ER) may be potential Eve. In [15], the authors investigated the joint trajectory and power control (PC) in power splitting enabled SWIPT networks.

Motivated by these observations, in this paper, the joint trajectories and PC in a dual-UAV enabled SWIPT network are investigated. Specifically, by treating ERs as the potential Eves, we aim to maximize the minimum secrecy rate among multiple LRs via jointly optimizing two UAV's trajectories and PC. Such consideration has not been investigated yet. To solve the formulated highly non-convex problem, we linearize the non-convex objective and constraints via SCA and CCCP. Then, an iterative method is proposed to solve the reformulated problem. Different from the AO method in relevant works, we do not decompose the original problem into subproblems. Instead, all the variables are optimized and updated integrally in every step during the iteration. Simulation results have demonstrated that the proposed algorithm achieves better performance than other algorithms.

The rest of this paper is organized as follows. The system model and problem statement are given in Section 2. Section 3 investigates the joint trajectories and PC design in dual-UAV enabled secrecy SWIPT networks. Simulation results are provided in Section 4. Section 5 concludes this paper.

2. SYSTEM MODEL AND PROBLEM STATEMENT

2.1. System Model

Let us consider a dual UAV-enabled SWIPT system, which consists of one communication UAV (UAV-C), one jamming UAV (UAV-J), several legitimate receivers (LRs), and several energy receivers (ERs). The confidential information sent from the UAV-C to the LRs may be eavesdropped by the ERs due to broadcast characteristics. The UAV-J transmits jamming signal to interfere the ERs, which may also act as an energy signal for the ERs. Without loss of generality (W.l.o.g), a three-dimensional (3D) Cartesian coordinate system with the ground is involved. The coordinates of the i -th LR and the k -th ER are denoted as $\mathbf{w}_{L_i} = [x_{L_i}, y_{L_i}]^T$, $\mathbf{w}_{E_k} = [x_{E_k}, y_{E_k}]^T$. The two UAVs are assumed to fly horizontally at a constant altitude H in m from the predetermined initial location $\mathbf{q}_{c_0} = [x_{c_0}, y_{c_0}]^T$ to the final location $\mathbf{q}_{c_F} = [x_{c_F}, y_{c_F}]^T$ in a finite time T . T is divided into N time slots with each slot duration $\delta_T = T/N$, which is small enough such that the UAV's location can be seen as a constant within each time slot, and the horizontal coordinates of the two UAVs in slot n are denoted as $\mathbf{q}_c[n] = [x_c[n], y_c[n]]^T$, $\mathbf{q}_j[n] = [x_j[n], y_j[n]]^T$, $n = 1, \dots, N$, respectively [5]. In addition, a practical case that there exist several no-fly zones (NFZ) in the possible trajectory is considered. The horizontal coordinate center and the radius of each NFZ are denoted by $\mathbf{q}_{NF}^m = [x_{NF}^m, y_{NF}^m]^T$ and D_m^2 , respectively [8].

Subject to the maximum speed constraints and the NFZ constraints, the UAV-C's trajectory should satisfy [8]

$$\|\mathbf{q}_c[1] - \mathbf{q}_{c_0}\|^2 \leq S_{\max}^2, \quad (1a)$$

$$\|\mathbf{q}_c[n+1] - \mathbf{q}_c[n]\|^2 \leq S_{\max}^2, \quad n = 1, \dots, N-1, \quad (1b)$$

$$\|\mathbf{q}_{c_F} - \mathbf{q}_c[N]\|^2 \leq S_{\max}^2, \quad (1c)$$

$$\|\mathbf{q}_c[n] - \mathbf{q}_{NF}^m\|^2 \geq D_m^2, \forall n, m, \quad (1d)$$

where $S_{\max} = V_{\max} \delta_T$ is the maximum horizontal distance that the UAV-C can travel within one time slot on the assumption of maximum speed V_{\max} in meter/second (m/s). Similarly, the UAV-J should also satisfy the speed constraints and NFZ constraints.

Following the commonly adopted free-space path loss model, the channel power gains from the two UAVs to the i -th LR and k -th ERs in time slot n are respectively given by [8]

$$a_i[n] = \frac{\gamma_0}{H^2 + \|\mathbf{q}_c[n] - \mathbf{w}_{L_i}\|^2}, \quad (2a)$$

$$b_k[n] = \frac{\gamma_0}{H^2 + \|\mathbf{q}_j[n] - \mathbf{w}_{L_i}\|^2}, \quad (2b)$$

$$c_k[n] = \frac{\gamma_0}{H^2 + \|\mathbf{q}_c[n] - \mathbf{w}_{E_k}\|^2}, \quad (2c)$$

$$d_k[n] = \frac{\gamma_0}{H^2 + \|\mathbf{q}_j[n] - \mathbf{w}_{E_k}\|^2}, \quad (2d)$$

where γ_0 denotes the channel power gain at the reference distance of 1 m, whose value is dependent on the antenna gain, carrier frequency, etc.

The transmit powers of the UAV-C and UAV-J in the n -th time slot are denoted by $P_c[n]$ and $P_j[n]$, respectively, subject to the following constraints [9]

$$\sum_{n=1}^N P_c[n] \leq N\bar{P}_c, 0 \leq P_c[n] \leq P_{cpeak}, \forall n, \quad (3a)$$

$$\sum_{n=1}^N P_j[n] \leq N\bar{P}_j, 0 \leq P_j[n] \leq P_{jpeak}, \forall n, \quad (3b)$$

where \bar{P}_c and P_{cpeak} denote the average power and peak power for the UAV-C, respectively, so the same to UAV-J.

On the ground, the received signals by the i -th LR and k -th ER are respectively given as follows [9]

$$y_{L_i}[n] = \sqrt{P_c[n]a_i[n]}s + \sqrt{P_j[n]b_i[n]}z + n_{L_i}, \quad (4a)$$

$$y_{E_k}[n] = \sqrt{P_c[n]c_k[n]}s + \sqrt{P_j[n]d_k[n]}z + n_{E_k}, \quad (4b)$$

where s is the information signal from the UAV-C; z is the jamming signal from the UAV-J; $n_{L_i} \sim \mathcal{CN}(0, \sigma_l^2)$ and $n_{E_k} \sim \mathcal{CN}(0, \sigma_e^2)$ are the noises at the LRs and ERs, respectively.

Similarly with the consideration in [9], we assume that the jamming signal z can be perfectly removed by the LRs. Thus, the signal-to-interference-noise-ratios (SINRs) for the i -th LR and k -th ER are respectively given by [9]

$$\Gamma_{L_i}[n] = \frac{P_c[n]a_i[n]}{\sigma_l^2}, \forall i, n \quad (5a)$$

$$\Gamma_{E_k}[n] = \frac{P_c[n]c_k[n]}{P_j[n]d_k[n] + \sigma_e^2}, \forall k, n. \quad (5b)$$

Accordingly, the secrecy rate for the dual-UAV enabled SWIPT network is given as follows [10]

$$R_s = \frac{1}{N} \sum_{n=1}^N \left[\min_{i \in \mathcal{I}} R_{L_i}[n] - \max_{k \in \mathcal{K}} R_{E_k}[n] \right]^+, \quad (6)$$

where $R_{L_i}[n]$ and $R_{E_k}[n]$ are the information rates for the i -th LR and k -th ER and the n -th slot, which are respectively given by [10],

$$R_{L_i}[n] = \log_2 \left(1 + \frac{P_c[n]a_i[n]}{\sigma_l^2} \right), \quad (7)$$

and

$$R_{E_k}[n] = \log_2 \left(1 + \frac{P_c[n]c_k[n]}{P_j[n]d_k[n] + \sigma_e^2} \right). \quad (8)$$

2.2. EH Constrained Secrecy Rate Maximization Design

In this paper, the joint trajectories, transmit power design is investigated. We aim to maximize the secrecy rate among these LRs, subject to the trajectories and transmit power constraints at the UAVs, as well as the EH constraints at the ERs. Mathematically, our problem is formulated as

$$\max_{\mathbf{P}_C, \mathbf{P}_J, \mathbf{q}_C, \mathbf{q}_J} R_s \quad (9a)$$

$$\text{s.t.} \quad (1a) - (1d), \quad (9b)$$

$$P_c[n]c_k[n] + P_j[n]d_k[n] \geq E_{th}, \forall n, k, \quad (9c)$$

where $\mathbf{q}_C \triangleq \{\mathbf{q}_c[n], \forall n\}$, $\mathbf{q}_J \triangleq \{\mathbf{q}_j[n], \forall n\}$, $\mathbf{P}_C \triangleq \{P_c[n], \forall n\}$, $\mathbf{P}_J \triangleq \{P_j[n], \forall n\}$, E_{th} is the minimum EH threshold for the ERs in each slot.

3. A JOINT DESIGN FOR THE SECRECY DUAL-UAV ENABLED SWIPT NETWORKS

The formulated problem is hard to handle due to multiply coupled variables and non-convex constraints [16]. In this section, we will propose a jointly trajectories and power design method.

Firstly, via introducing auxiliary variables φ_k and ψ_k , Eq. (9c) can be reformulated as follows

$$\frac{P_c[n]\gamma_0}{\varphi_k[n]} + \frac{P_j[n]\gamma_0}{\psi_k[n]} \geq E_{th}, \quad (10a)$$

$$H^2 + \|\mathbf{q}_c[n] - \mathbf{w}_{E_k}\|^2 \leq \varphi_k[n], \forall n, k, \quad (10b)$$

$$H^2 + \|\mathbf{q}_j[n] - \mathbf{w}_{E_k}\|^2 \leq \psi_k[n], \forall n, k. \quad (10c)$$

However, Eq. (10a) is still non-convex. In the following, the first-order approximation will be utilized to handle these constraints. Specifically, by denoting $P_c^r[n]$, $P_j^r[n]$, $\varphi_k^r[n]$, and $\psi_k^r[n]$ as the optimal $P_c[n]$, $P_j[n]$, $\varphi_k[n]$, and $\psi_k[n]$ at the r -th iteration, the first part of the left hand side of Eq. (10a) can be approximated as

$$\frac{P_c[n]}{\varphi_k[n]} \geq \frac{P_c^r[n]}{\varphi_k^r[n]} + \frac{P_c[n] - P_c^r[n]}{\varphi_k^r[n]} - \frac{P_c^r[n](\varphi_k[n] - \varphi_k^r[n])}{(\varphi_k^r[n])^2} = \frac{P_c^r[n] + P_c[n]}{\varphi_k^r[n]} - \frac{P_c^r[n]\varphi_k[n]}{(\varphi_k^r[n])^2}, \quad (11)$$

Similarly, we have

$$\frac{P_j[n]}{\psi_k[n]} \geq \frac{P_j^r[n] + P_j[n]}{\psi_k^r[n]} - \frac{P_j^r[n]\psi_k[n]}{(\psi_k^r[n])^2}. \quad (12)$$

Thus, Eq. (9c) can be approximated as

$$\frac{P_c^r[n] + P_c[n]}{\varphi_k^r[n]} - \frac{P_c^r[n]\varphi_k[n]}{(\varphi_k^r[n])^2} + \frac{P_j^r[n] + P_j[n]}{\psi_k^r[n]} - \frac{P_j^r[n]\psi_k[n]}{(\psi_k^r[n])^2} \geq E_{th}, \forall n, k, \quad (13)$$

Then, we will focus on the objective. By invoking some slack variables, the objective can be rewritten as follows

$$\max \sum_{n=1}^N \alpha[n] - \beta[n] \quad (14a)$$

$$\text{s.t. } \frac{P_c[n]}{H^2 + \|\mathbf{q}_c[n] - \mathbf{w}_{L_i}\|^2} \geq (2^{\alpha[n]} - 1) \sigma_l^2, \forall n, i, \quad (14b)$$

$$\frac{\vartheta_k[n]}{\zeta_k[n] + \sigma_e^2} \leq 2^{\beta[n]} - 1, \forall n, k, \quad (14c)$$

$$\frac{P_c[n]}{H^2 + \|\mathbf{q}_c[n] - \mathbf{w}_{E_k}\|^2} \leq \vartheta_k[n], \forall n, k, \quad (14d)$$

$$\frac{P_j[n]}{H^2 + \|\mathbf{q}_j[n] - \mathbf{w}_{E_k}\|^2} \geq \zeta_k[n], \forall n, k, \quad (14e)$$

where $\alpha[n], \forall n$, $\beta[n], \forall n$, $\vartheta_k[n], \forall k, n$, and $\zeta_k[n], \forall k, n$ are introduced variables.

However, Eq. (14) still has multiply non-convex constraints. Firstly, we focus on Eq. (14b). In fact, Eq. (14b) can be further rewritten as

$$\frac{P_c[n]}{H^2 + \|\mathbf{q}_c[n] - \mathbf{w}_{L_i}\|^2} \geq \mu_i[n], \forall i, n, \quad (15a)$$

$$\mu_i[n] \geq (2^{\alpha[n]} - 1) \sigma_l^2, \forall i, n, \quad (15b)$$

$$H^2 + \|\mathbf{q}_c[n] - \mathbf{w}_{L_i}\|^2 \leq \kappa_i[n], \forall i, n \quad (15c)$$

$$P_c[n] \geq \mu_i[n]\kappa_i[n], \forall i, n. \quad (15d)$$

In addition, Eq. (14c) can be rewritten as follows

$$\frac{\vartheta_k[n]}{2^{\beta[n]} - 1} \leq \zeta_k[n] + \sigma_e^2, \forall k, n. \quad (16)$$

Next, to turn Eq. (15d) into a solvable reformulation, we introduce the following lemma.

Lemma 1 [17]: Function in the form $\xi(x, y) = xy$ is quasi-concave. For arbitrary $\mu > 0$, let us define a function

$$\xi_u(x, y) = \frac{u}{2}x^2 + \frac{1}{2u}y^2,$$

then $\xi_u(x, y)$ is always an upper estimate of $\xi(x, y)$ for a fixed $\mu > 0$, and it is convex. Furthermore, $\xi_u(x, y)$ also satisfies

$$\xi_u(x, y) = \xi(x, y), \quad \nabla \xi_u(x, y) = \nabla \xi(x, y),$$

when $u = y/x$.

Via the above lemma and introduce auxiliary variables $\varpi_i[n], \forall i, n$, Eq. (15d) can be reformulated as

$$P_c[n] \geq \frac{\varpi_i[n]}{2}\mu_i^2[n] + \frac{1}{2\varpi_i[n]}\kappa_i^2[n], \forall i, n. \quad (17)$$

Then we will focus on Eq. (16). Via introducing slack variables $\omega_k[n], \forall k, n$, Eq. (16) is equivalently to the following constraints

$$\vartheta_k[n]\omega_k[n] \leq \zeta_k[n] + \sigma_e^2, \forall k, n, \quad (18)$$

$$\frac{1}{\omega_k[n]} + 1 \leq 2^{\beta[n]}, \forall k, n. \quad (19)$$

Similarly, via Lemma 1 and introduce slack variables $\chi_k[n], \forall k, n$, Eq. (18) can be further approximated as

$$\frac{\chi_k[n]}{2}\vartheta_k^2[n] + \frac{1}{2\chi_k[n]}\omega_k^2[n] \leq \zeta_k[n] + \sigma_e^2, \forall k, n, \quad (20)$$

while Eq. (19) can be approximated as the following first order Taylor expansion

$$\frac{1}{\omega_k[n]} + 1 \leq 2^{\beta^r[n]}(\beta[n] - \beta^r[n] + 1), \forall k, n. \quad (21)$$

In the following, we will handle Eq. (14d). In fact, Eq. (14d) can be rewritten as the following two constraints

$$P_c[n]\varsigma_k[n] \leq H^2 + \|\mathbf{q}_c[n] - \mathbf{w}_{E_k}\|^2, \forall k, n, \quad (22a)$$

$$\frac{1}{\vartheta_k[n]} \leq \varsigma_k[n] \Rightarrow 1 \leq \vartheta_k[n]\varsigma_k[n], \forall k, n. \quad (22b)$$

where $\varsigma_k[n], \forall k, n$ are introduced slack variables.

The main obstacle lies in Eq. (22a). Via Lemma 1 and following a similar way to that in [5], Eq. (22a) can be approximated as

$$\frac{\delta_k[n]}{2}P_c^2[n] + \frac{1}{2\delta_k[n]}\varsigma_k^2[n] \leq H^2 + \|\mathbf{q}_c^r[n] - \mathbf{w}_{E_k}\|^2 + 2\|\mathbf{q}_c^r[n] - \mathbf{w}_{E_k}\|^T \|\mathbf{q}_c[n] - \mathbf{q}_c^r[n]\|, \forall k, n, \quad (23)$$

where $\delta_k[n], \forall k, n$ are introduced slack variables.

In addition, the product term $\vartheta_k[n]\varsigma_k[n]$ in Eq. (22b) can be recast as the following second-order cone (SOC) formulation

$$\vartheta_k[n]\varsigma_k[n] = \frac{1}{4}(\vartheta_k[n] + \varsigma_k[n])^2 - \frac{1}{4}(\vartheta_k[n] - \varsigma_k[n])^2. \quad (24)$$

Thus, Eq. (22b) can be turned into the following SOC constraint

$$\| 2 \vartheta_k[n] - \varsigma_k[n] \| \leq \vartheta_k[n] + \varsigma_k[n], \forall k, n. \quad (25)$$

Next, we will focus on Eq. (14e). Firstly, Eq. (14e) can be recast as

$$\frac{P_j[n]}{\zeta_k[n]} \geq H^2 + \|\mathbf{q}_j[n] - \mathbf{w}_{E_k}\|^2, \forall k, n. \quad (26)$$

Via introducing auxiliary variables $\pi_k[n], \forall k, n$, Eq. (26) is equivalent to

$$P_j[n] \geq \pi_k[n]\zeta_k[n], \forall k, n, \quad (27a)$$

$$\pi_k[n] \geq H^2 + \|\mathbf{q}_j[n] - \mathbf{w}_{E_k}\|^2, \forall k, n, \quad (27b)$$

while Eq. (27a) is approximated as

$$P_j[n] \geq \frac{\iota_k[n]}{2} \pi_k^2[n] + \frac{1}{2\iota_k[n]} \zeta_k^2[n], \forall k, n, \quad (28)$$

where $\iota_k[n], \forall k, n$ are introduced slack variables.

At last, following a similar way to that in [4], the NFZ constraints can be approximated as

$$\|\mathbf{q}_c[n] - \mathbf{q}_{NF}^m\|^2 \geq \|\mathbf{q}_c^r[n] - \mathbf{q}_{NF}^m\|^2 + 2(\mathbf{q}_c^r[n] - \mathbf{q}_{NF}^m)^T (\mathbf{q}_c[n] - \mathbf{q}_c^r[n]) \geq D_m^2, \forall m, n. \quad (29)$$

Combining these steps, at given point $\{P_c^r[n], P_j^r[n], \mathbf{q}_c^r[n], \mathbf{q}_j^r[n]\}$, we obtain the following equivalent problem

$$\max \sum_{n=1}^N \alpha[n] - \beta[n] \quad (30a)$$

$$\text{s.t. (1a) - (1c), (10b), (10c), (13), (15b), (15c),} \quad (30b)$$

$$(17), (20), (21), (23), (25), (27b), (28), (29), \quad (30c)$$

which can be efficiently solved by the convex programming toolbox CVX [18].

To this end, we have transformed Eq. (9) into a convex approximated problem, which can be solved in an iterative way.

4. NUMERICAL RESULTS

In this section, we provide some Monte-Carlo (MC) simulations to testify the availability of our proposed scheme. Unless specified, the simulation setting is assumed as follows: The maximum flying speed is $V_{\max} = 30m/s$, and the flying altitude is set to $H = 100$ m. The horizontal coordinates of the UAVs' initial and final locations are set as $\mathbf{q}_0 = [0, 300]^T$ and $\mathbf{q}_F = [0, -300]^T$, respectively. There are two LRs and two ERs in the SWIPT system. The LRs are located at $[-200, -20]^T$ and $[-200, 20]^T$, respectively. The ERs are located at $[200, -20]^T$ and $[200, 20]^T$, respectively. We set $T = 60$ s, $\delta_T = 0.5$ s, $\gamma_0 = 60$ dB, $P_{cpeak} = 4\bar{P}_c$, $\bar{P}_c = -30$ dBw, and $E_{th} = -70$ dBw. In addition, we compare our proposed design with the following methods: 1) the dual UAV's trajectory and PC method in [9], without considering the EH constraint; 2) the no jamming UAV case in [14], e.g., there is only the UAV-C; 3) the no PC case, e.g., only optimizing the trajectories with fixed transmit power; 4) the proposed design without the NFZ constraint. These methods are denoted as "the proposed method", "the no EH case in [9]", "the no UAV-J case in [14]", "the no PC case", and "the no NFZ case", respectively.

Firstly, we show the trajectories of the two UAVs for different methods in a given scenario in Fig. 1. The LRs, ERs, and UAVs' initial and final locations are marked with \circ , Δ , \times , and $+$, respectively. The trajectories of these methods are shown in different colours, while full line and dotted line denote the UAV-C's trajectory and UAV-J's trajectory with a given method, respectively. From this figure, we can see that the trajectory of the proposed method stays away from the NFZ. In addition, the optimal trajectory for UAV-J in fact passes through the NFZ, which shows the effect of the NFZ in the trajectory design.

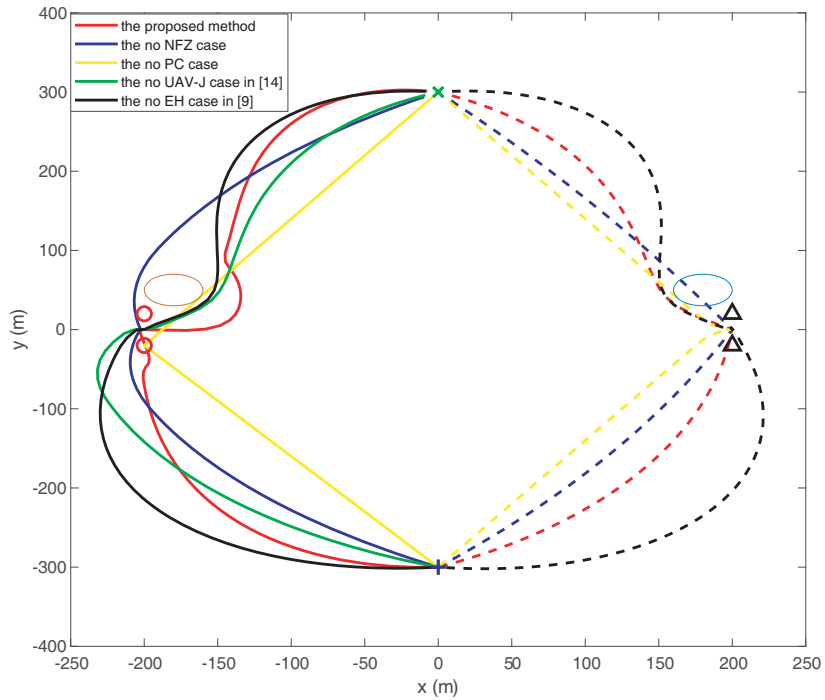


Figure 1. The UAVs’ trajectories for different methods.

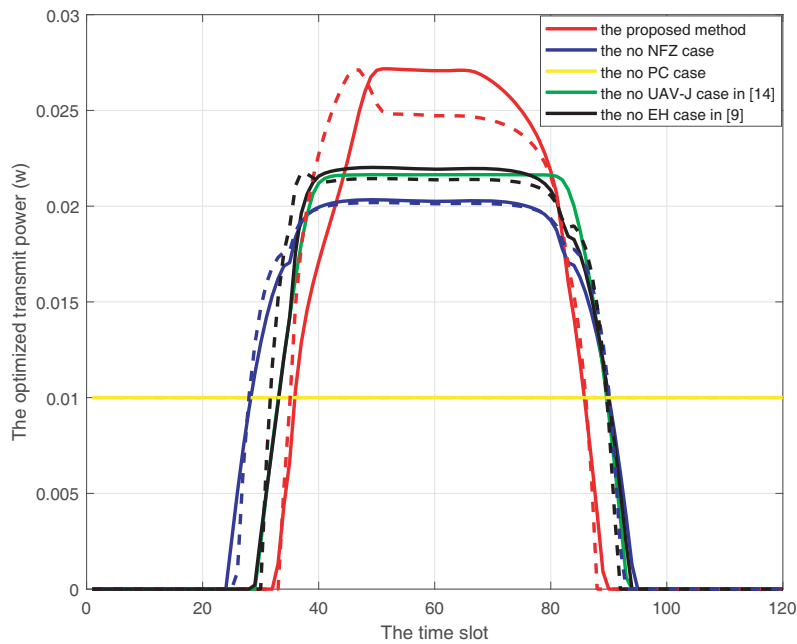


Figure 2. The UAVs’ transmit power for different methods.

Secondly, we show the relationship between the UAVs’ transmit power and the time slot for these methods, while full line and dotted line denote the UAV-C’s transmit power and UAV-J’s transmit power with a given method, respectively. It can be observed from Fig. 2 that the transmit power is closely correlated with the trajectories of the two UAVs, which implies the necessity of joint trajectory optimization and power allocation. In addition, the transmit power of the two UAVs tends to increase

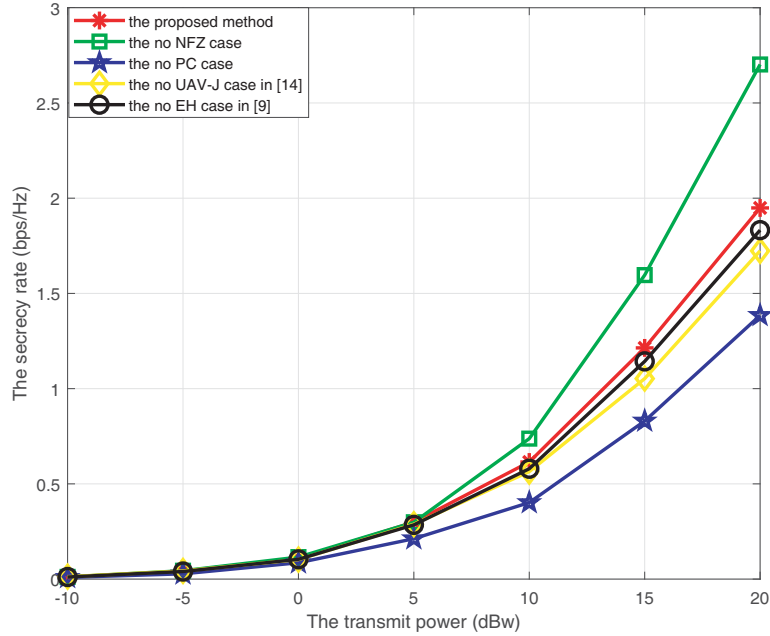


Figure 3. The secrecy rate versus the average transmit power.

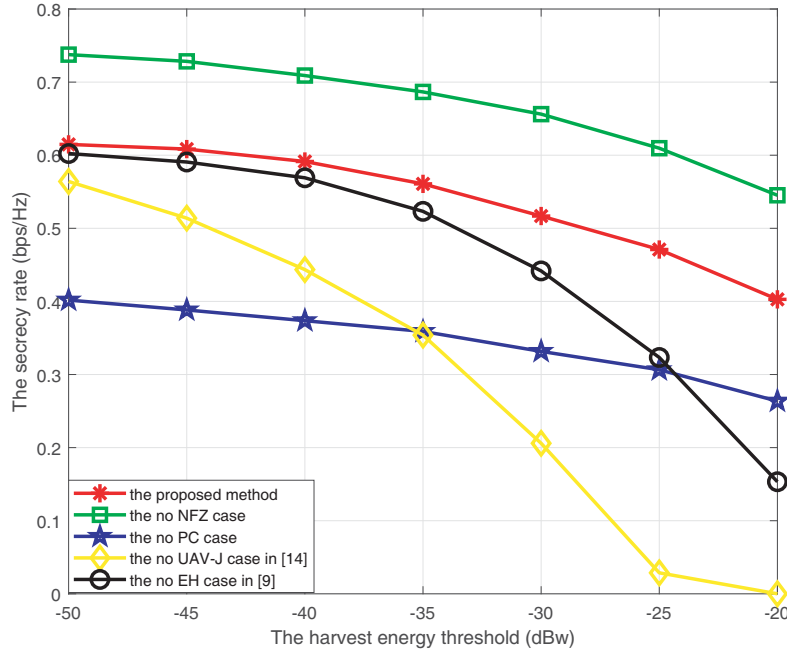


Figure 4. The secrecy rate versus the ER's EH threshold.

when the UAVs fly close to the target, which coincides with the results in related works such as [11] and [12].

Thirdly, we show the secrecy rate versus the average power \bar{P}_c for these methods. From Fig. 3, we can see that R_s increases with the increase of \bar{P}_c . Our method outperforms the other designs, while the no NFZ case achieves the best performance, which demonstrates the effect of NFZ on a UAV network.

Lastly, we show the secrecy rate versus EH threshold E_{th} for these methods. From Fig. 4, we can see that R_s decreases with the increase of E_{th} . In addition, when E_{th} is relatively low, no jamming

design outperforms no PC design. However, when E_{th} is relatively high, no PC design outperforms no jamming design. In addition, the design in [9] suffers from performance loss in high E_{th} region, since [9] is not involved with energy harvesting.

5. CONCLUSION

In this paper, the joint optimization of trajectories and PC for a dual-UAV enabled secrecy SWIPT system has been investigated. We formulate the problem to maximize the minimum secrecy rate among the LRs under trajectory constraints and power constraints. In order to tackle the highly non-convex problem, we utilize CCCP and SCA to reformulate a solvable convex problem. The simulation results demonstrate that the proposed algorithm achieves better performance than other designs.

ACKNOWLEDGMENT

This work was partly supported by the National Natural Science Foundation of China under Grant No. 61673108, partly supported by the Colleges and Universities Natural Science Foundation in Jiangsu Province under contracts No. 18KJD510010 and No. 19KJA110002, partly supported by the industry-university-research cooperation project of Jiangsu province under Grant No. BY2018282, partly supported by the Open Project Program of the Key Laboratory of Underwater Acoustic Signal Processing, Ministry of Education, China under contracts No. UASP1801, and partly supported by the Fundamental Research Funds for the Central Universities under contracts No. 2242016K30013.

REFERENCES

1. Kawamoto, Y., H. Nishiyama, N. Kato, F. Ono, and R. Miura, "Toward future unmanned aerial vehicle networks: Architecture, resource allocation and field experiments," *IEEE Wireless Commun.*, Vol. 26, No. 1, 94–99, Feb. 2019.
2. Li, B., Z. Fei, and Y. Zhang, "UAV communications for 5G and beyond: Recent advances and future trends," *IEEE Inter. Things Jour.*, Vol. 6, No. 2, 2241–2263, Apr. 2019.
3. He, D., S. Chan, and M. Guizani, "Communication security of unmanned aerial vehicles," *IEEE Wireless Commun.*, Vol. 24, No. 4, 134–139, Aug. 2017.
4. Tang, H., Q. Wu, and B. Li, "An efficient solution for joint power and trajectory optimization in UAV-enabled wireless network," *IEEE Access*, Vol. 7, 59640–59625, Mar. 2019.
5. Zhang, G., Q. Wu, M. Cui, and R. Zhang, "Securing UAV communications via joint trajectory and power control," *IEEE Trans. Wireless Commun.*, Vol. 18, No. 2, 1376–1389, Feb. 2019.
6. Cui, M., G. Zhang, Q. Wu, and D. W. K. Ng, "Robust trajectory and transmit power design for secure UAV communications," *IEEE Trans. Veh. Tech.*, Vol. 67, No. 9, 9042–9046, Sep. 2018.
7. Zhou, X., Q. Wu, S. Yan, F. Shu, and J. Li, "UAV-enabled secure communications: Joint trajectory and transmit power optimization," *IEEE Trans. Veh. Tech.*, Vol. 68, No. 4, 4069–4073, Apr. 2019.
8. Gao, Y., H. Tang, B. Li, and X. Yuan, "Joint trajectory and power design for UAV-enabled secure communications with no-fly zone constraints," *IEEE Access*, Vol. 7, 44459–44470, Apr. 2019.
9. Cai, Y., F. Cui, Q. Shi, M. Zhao, and G. Y. Li, "Dual-UAV-enabled secure communications: Joint trajectory design and user scheduling," *IEEE J. Sel. A. Commun.*, Vol. 36, No. 9, 1972–1985, Sep. 2018.
10. Lee, H., S. Eom, J. Park, and I. Lee, "UAV-aided secure communications with cooperative jamming," *IEEE Trans. Veh. Tech.*, Vol. 67, No. 10, 9385–9392, Oct. 2018.
11. Zhong, C., J. Yao, and J. Xu, "Secure UAV communication with cooperative jamming and trajectory control," *IEEE Commun. Lett.*, Vol. 23, No. 2, 286–289, Feb. 2019.
12. Li, A., Q. Wu, and R. Zhang, "UAV-enabled cooperative jamming for improving secrecy of ground wiretap channel," *IEEE Wireless Commun. Lett.*, Vol. 8, No. 1, 181–184, Feb. 2019.

13. Perera, T., D. Jayakody, S. Sharma, S. Chatzinotas, and J. Li, “Simultaneous wireless information and power transfer (SWIPT): Recent advances and future challenges,” *IEEE Commun. Surv. Tut.*, Vol. 20, No. 1, 264–302, Quart. 1st, 2018.
14. Hong, X., P. Liu, F. Zhou, S. Guo, and Z. Chu, “Resource allocation for secure UAV-assisted SWIPT systems,” *IEEE Access*, Vol. 7, 24248–24257, Feb. 2019.
15. Huang, F., J. Chen, H. Wang, G. Ding, Z. Xue, Y. Yang, and F. Song, “UAV-assisted SWIPT in internet of things with power splitting: Trajectory design and power allocation,” *IEEE Access*, Vol. 7, 68260–68270, Jun. 2019.
16. Boyd, S. and L. Vandenberghe, *Convex Optimization*, Cambridge Univ. Press, Cambridge, UK, 2004.
17. Gao, H., T. Lv, W. Wang, and N. C. Beaulieu, “Energy-efficient and secure beamforming for self-sustainable relay-aided multicast networks,” *IEEE Signal Process. Lett.*, Vol. 23, No. 11, 1509–1513, Nov. 2016.
18. Grant, M. and S. Boyd, CVX: Matlab software for disciplined convex programming, version 2.0 beta, Sep. 2012, Available: <http://cvxr.com/cvx>.